Tectonophysics, 128 (1986) 335–356
Elsevier Science Publishers B.V., Amsterdam – Printed in The Netherlands

HEAT FLOW, HEAT PRODUCTION AND FISSION TRACK DATA FROM THE HERCYNIAN BASEMENT AROUND THE PROVENÇAL BASIN (WESTERN MEDITERRANEAN)

F. LUCAZEAU [1] and D. MAILHE [2]

[1] *Centre Géologique et Géophysique, Université des Sciences et Techniques du Languedoc, Montpellier (France)*
[2] *Centre des Faibles Radioactivités, Laboratoire mixte CEA-CNRS, Gif sur Yvette (France)*

(Received December 3, 1985; accepted March 21, 1986)

ABSTRACT

Lucazeau, F. and Mailhé, D., 1986. Heat flow, heat production and fission track data from the Hercynian basement around the Provençal Basin (Western Mediterranean). In: D.A. Galson and St. Mueller (Editors), The European Geotraverse, Part 2. *Tectonophysics*, 128: 335–356.

In the complex structural framework of the Western Mediterranean, Hercynian areas are expected to be thermally preserved from the recent tectonic evolution. The thermal regime of these areas is studied using heat flow, heat production and fission track data. The surface heat flow is significantly higher in Corsica (76 ± 10 mW m^{-2}) than in the Maures and Estérel (58 ± 2 mW m^{-2}). Neither heat production nor erosion subsequent to the Alpine orogeny in Corsica can explain such a difference. It is suggested that a deep thermal source related to the asymmetric evolution of the Provençal basin could explain the higher heat flow in Corsica. A model of thermal structure based on the present day thermal regime of the Maures and Estérel is proposed for the stable Hercynian crust in this area. The mantle heat flow is 20–25 mW m^{-2} and the temperature at Moho level is 375–500°C, depending on the thermal parameter distribution with depth.

INTRODUCTION

In the framework of European Geotraverse (EGT), geothermal studies have been undertaken in order to evaluate the surface heat flow and the temperature field within the lithosphere. The area encompassing the Southern Segment of the EGT belongs to the Western Mediterranean domain where both Alpine structures and young oceanic crust exist. In such a context, heat transfer is time dependent and evaluation of the temperature field requires thermal modelling of the transient processes (uplift and erosion, rifting and oceanic accretion, sedimentation, etc.). Nevertheless, there exist few areas in the Western Mediterranean where Hercynian basement outcrops, which could be used to obtain a reference thermal state for this modelling work. In this paper, interest is focused on the thermal regime of the

0040-1951/86/$03.50

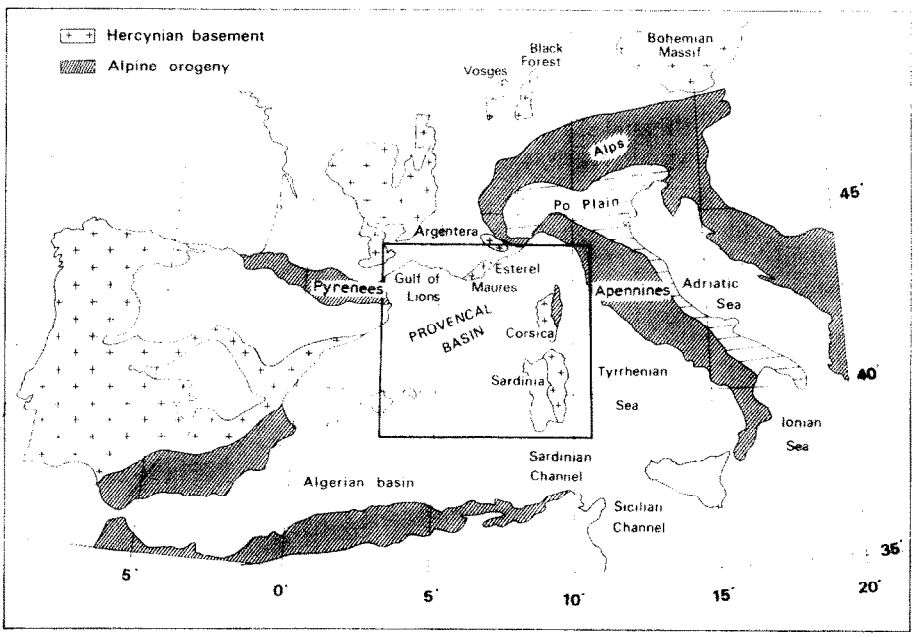

Fig. 1. Locations of the Provençal Basin and the Hercynian basement in the Western Mediterranean. Crosses indicate the Hercynian outcrops, shaded areas indicate the Alpine orogenic zones.

Hercynian, outer parts of the Provençal Basin (northwest Mediterranean): Maures and Estérel in the southern part of France, and Corsica and Sardinia (Fig. 1).

The Provençal Basin was formed during the Oligocene by rifting of the continental lithosphere (Biju-Duval et al., 1978), and then by oceanic accretion which shifted the Corsica–Sardinia block away from France (Burrus, 1984). In this Basin, the continental crust is progressively thinned to about 5–6 km (Le Douaran et al., 1984) whereas crustal thickness is normal in the Maures (Recq, 1970), in Corsica (Hirn and Sapin, 1977), and in Sardinia (Egger et al., 1985). Therefore, these areas were probably not affected by either Alpine orogeny or continental rifting.

The thermal regime of the Hercynian crust is discussed using heat flow and heat production data from Maures–Estérel and Corsica. Fission track data are used to make sure that erosion processes have not perturbed the temperature field. A contour map of heat flow in the Western Mediterranean, resulting from a compilation of all existing data, is presented in the final discussion of the paper. Also presented is a model for stable Hercynian crust based on the present-day thermal regime of the Maures and Estérel.

HEAT FLOW DATA

In Corsica, 11 data have been previously published by Lesquer et al. (1983), and are gathered in this paper with nine new measurements. In Maures-Estérel, seven

new measurements are presented. Temperature surveys were carried out with a thermistor probe giving a relative accuracy of 0.01°C. Temperature profiles were corrected to account for topographic effects according to the classical procedure (Balling et al., 1981). No other correction was applied to the data. Conductivity measurements were made on water-saturated half-cores with a transient method of determination.

Heat flow from Corsica

All of the data were obtained in shallow boreholes drilled for water resources, but only unproductive boreholes were used. Temperature profiles are displayed in Fig. 2; most of them have a curvature, which can be explained in some cases by thermal conductivity contrasts (Partinello) or water circulation (Casavecchie, Lama 24 and Luri 38). In other boreholes, there is no evidence for water circulation to explain this curvature. However, for the most reliable data (Piattone, Alata, Lama 26), the variation of the thermal gradient within the borehole does not exceed 5°C km^{-1}. For all of the boreholes in the Hercynian basement, the standard deviation on the average gradient (24.5 ± 4.5°C km^{-1}) is of the same order of magnitude. This

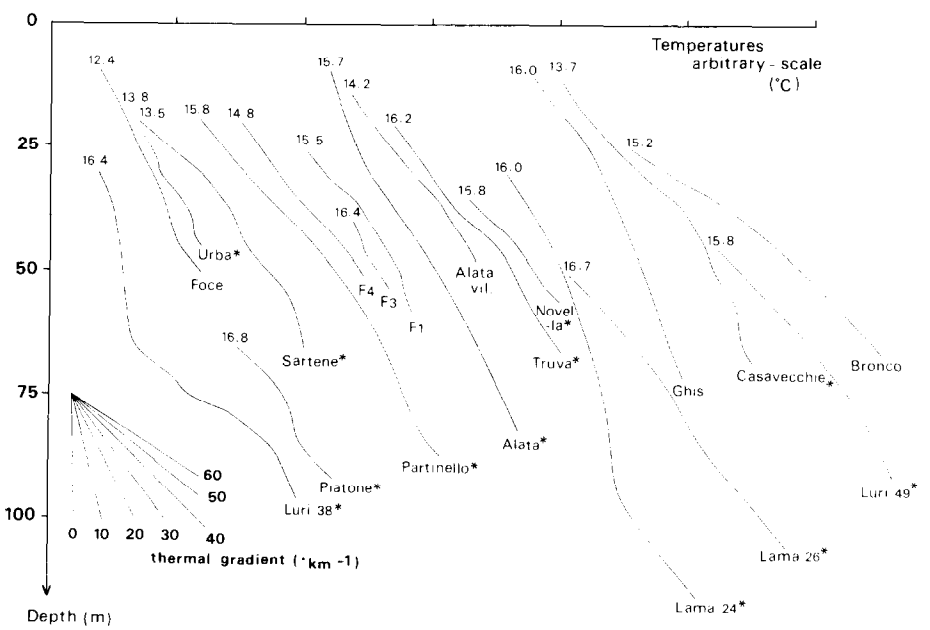

Fig. 2. Temperature profiles versus depth for the various boreholes logged in Corsica. Temperatures are represented using an arbitrary scale, one division representing one degree. The value on the upper part of each profile represents the actual temperature at the depth for which the thermal log begins. The stars correspond to data already published by Lesquer et al. (1983).

TABLE 1

Heat flow data from Corsica *

Locality	Long. E	Lat. N	Depth range (m)	Conductivity (W m^{-1} °C^{-1})	Thermal gradient (°C km^{-1})	Heat flow ** uc (mW m^{-2})	Heat flow ** ct (mW m^{-2})	Lithology
North Alpine Corsica — average heat flow = 82 ± 12 mW m^{-2}								
Luri 38 [a]	9°24′	42°58′	65–90	2.45	38.4	94	94	schist
Luri 49 [a]	9°24′	42°58′	20–75	2.45	20.6	83	70	schist
South Alpine Corsica — average heat flow = 81 ± 19 mW m^{-2}								
Casavecchie [a]	9°22′	42°08′	10–70	2.42	20.1	111	100	schist
Ghisonaccia	9°23′	41°57′	20–70	4.0 [b]	15.6	62	62	sandstone
Tenda massif — average heat flow = 78 ± 7 mW m^{-2}								
Novella [a]	9°09′	42°35′	30–65	2.5 [b]	32.8	89	84	flysch
Lama 26 [a]	9°09′	42°34′	30–105	2.5 [b]	33.8	103	71	spilite
Lama 24 [a]	9°10′	42°34′	30–120	2.9	27	75	78	granite
Osani area — average heat flow = 74 ± 2 mW m^{-2}								
Partinello [a]	8°40′	42°18′	20–90	2.5 [b]	37	92	76	rhyolite
				3.0 [b]	20	59		granite
Osani F4	8°38′	42°19′	20–50	3.0 [b]	32.8	132	98	granite
Osani F1	8°39′	42°19′	35–60	3.0 [b]	24.0	86	72	granite
Osani F3	8°38′	42°19′	15–52	1.4 [b]	66	108	92	carbon
				3.6 [b]	20			schist
Ajaccio area — average value = 64 ± 3 mW m^{-2}								
Alata	8°45′	41°58′	10–82	3.0 [b]	22.4	56	67	granite
Alata 2	8°45′	41°58′	15–48	3.0 [b]	31.2	92	94	granite
Truva [a]	8°46′	41°58′	10–70	2.5 [b]	24.4	72	61	gabbro
South Ajaccio area — average heat flow = 75 ± 2 mW m^{-2}								
Foce	9°01′	41°37′	10–50	3.0 [b]	17.6	53	60	granite
Urbalacone [a]	8°57′	41°50′	20–45	2.9	24.8	76	72	granite
Piattone [a]	8°54′	41°45′	60–91	3.0 [b]	24.0	72	72	granite
Sartene [a]	8°59′	41°35′	25–65	3.0 [b]	25.6	84	77	granite
Bronco	8°50′	41°46′	30–74	3.0 [b]	44.0	148	132	granite

* Average heat flow values calculated only for boreholes deeper than 60 m.

** uc = uncorrected values; ct = corrected for topographic effects.

[a] Value previously published by Lesquer et al. (1983). [b] Estimated value.

suggests that all of the data are consistent despite the shallow depths and the uncertainties for individual values of thermal gradient. None of these boreholes have been cored and conductivities were estimated from measurements on surface samples. Heat flow values are presented in Table 1. The average value is 76 ± 16 mW m^{-2} for all of the data and 76 ± 10 mW m^{-2} for boreholes deeper than 60 m. This value is therefore representative of the surface heat flow in Corsica, but local

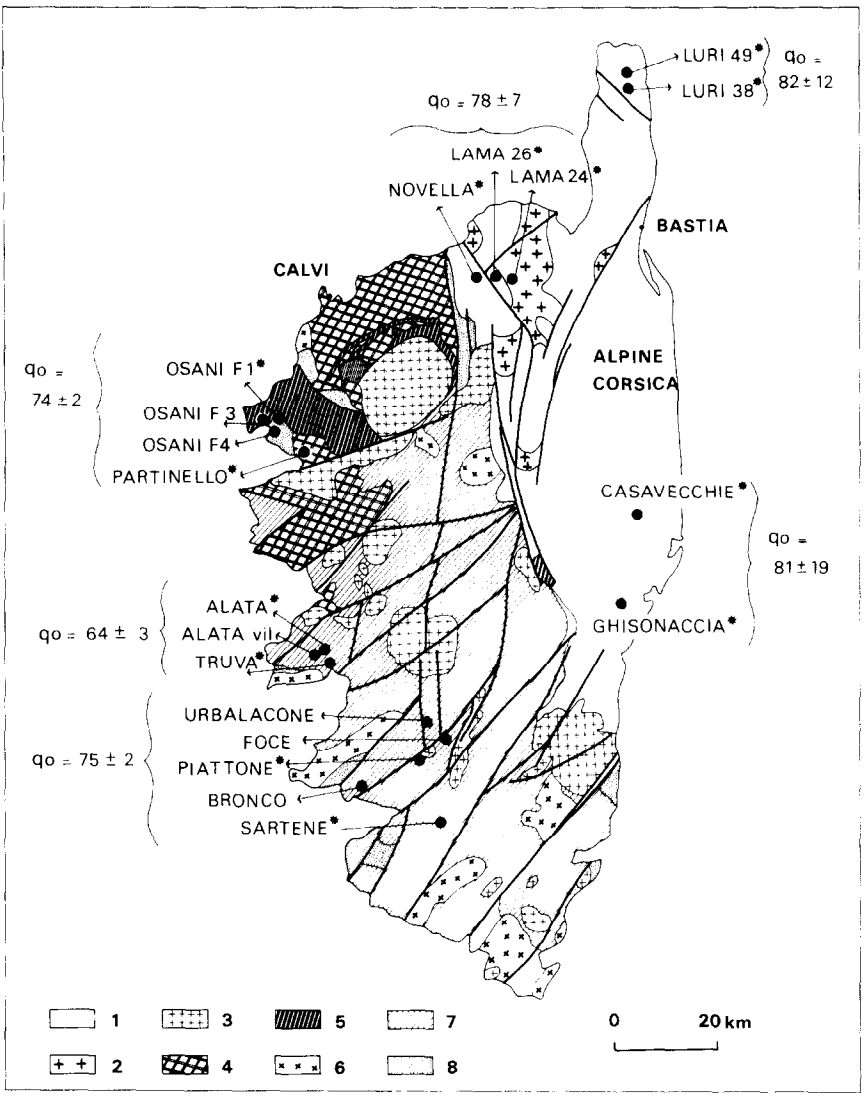

Fig. 3. Estimated heat flow for different provinces of Corsica, superposed on the geological map. Large dots represent heat flow measurements. Stars indicate boreholes deeper than 60 m used in the averaging. *1* = post-Hercynian, *2* = Hercynian granite of Tenda (Alpine Corsica), *3* = Permian anorogenic granite, *4* = subalkaline granite, *5* = Permian rhyolite, *6* = leucocratic granite, *7* = calk-alkaline granite, *8* = metamorphic basement.

variations can be expected for the different structural units (Fig. 3 and Table 1). Alpine Corsica, both on the Mesozoic unit and on the Hercynian unit of Tenda, has a slightly higher heat flow (80 mW m^{-2}). On the other hand, the Ajaccio area is characterized by a lower heat flow (64 mW m^{-2}).

Heat flow from the Maures and Estérel

In southern France, seven new data are available: two in the Maures, two in Estérel and three in the vicinity of the Hercynian basement. Temperature profiles are presented in Fig. 4; they are obviously more regular than those of Corsica, and boreholes are deeper. Heat flow values are given in Table 2 and Fig. 5. The two boreholes from Estérel (Castelli and Gratadis) have been drilled for mining research in the Permian rhyolites. Heat flow values obtained in these two boreholes (respectively 56 and 58 mW m^{-2}) correspond to reliable data according to the EGT criterion (depth greater than 100 m, conductivity measurements on several cores along the borehole, borehole free of water circulation, etc.). The two boreholes from the Maures (Ramatuelle and Cogolin) are shallower and conductivities were estimated from surface samples. However, heat flow values (respectively 61 and 59 mW

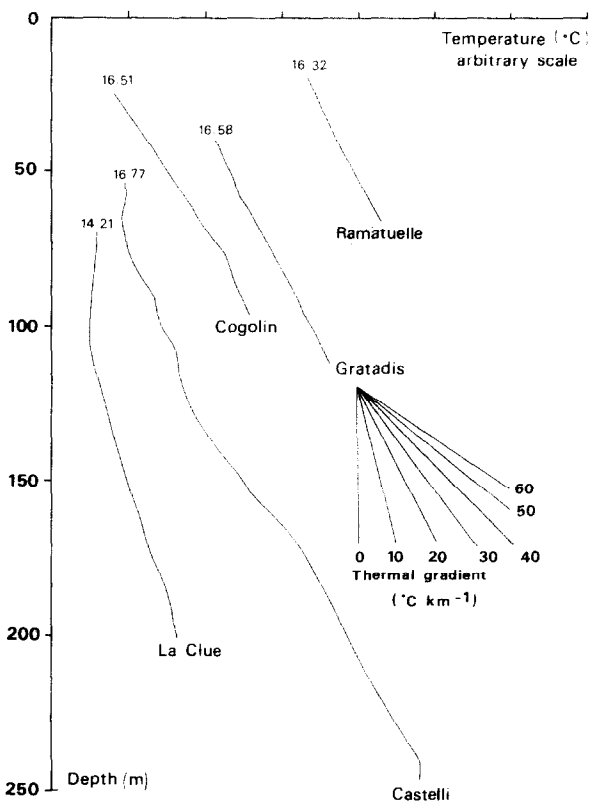

Fig. 4. Temperature profiles versus depth for the various boreholes logged in Maures and Estérel. Temperatures are represented using an arbitrary scale, one division representing one degree. The value on the upper part of each profile represents the actual temperature at the depth at which the thermal log begins.

TABLE 2

Heat flow data from Maures–Estérel

Locality	Long. E	Lat. N	Depth range (m)	Conductivity ($W\ m^{-1}\ °C^{-1}$)	Thermal gradient ($°C\ km^{-1}$)	Heat flow *		Lithology
						uc ($mW\ m^{-2}$)	ct ($mW\ m^{-2}$)	
Maures								
Ramatuelle	6°34	43°15′	20–65	3.0	20.4	61	61	schist
Cogolin	6°32	43°15′	25–95	2.7	25.6	69	59	gneiss
					17.6	48		
Estérel								
Castelli	6°50′	43°28′	50–250	1.9	32.0	62	58	pelite
				2.7	22.0			rhyolite
Gratadis	6°52′	43°28′	30–125	2.65	21.0	66	56	rhyolite
Vicinity of Estérel-Maures								
La Clue	6°31′	43°34′	100–200	3.91	14.5	57	57	dolomite
Gardanne	5°17′	43°30′	100–1000	2.36	24.5	61	58	limestone
Carces	6°07′	43°28′	0–1692	2.24 [a]	23	51	54	oil data

* uc = uncorrected values; ct = corrected for topographic effects.

[a] Estimated value.

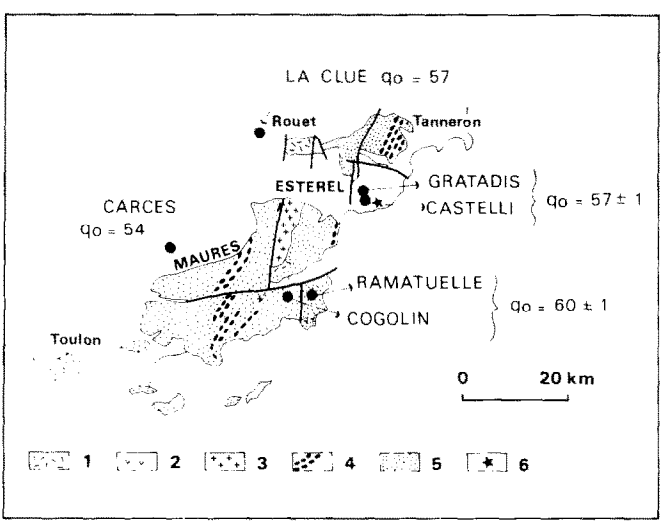

Fig. 5. Estimated heat flow from Maures and Estérel. *1* = diorite, *2* = leucogranite, *3* = cordierite-granite, *4* = granite–gneiss, *5* = metamorphic schist, gneiss and anatectic gneiss, *6* = estérellite.

m^{-2}) are consistent with values obtained in Estérel. Three other measurements have been obtained in the vicinity of the Hercynian basement of Provence and confirm values from the Maures and Estérel. One of these data (Carcès) corresponds to an oil exploration borehole, for which one BHT measurement was available at the bottom and was corrected for mud circulation effects. The average value in this area (58 ± 2 mW m^{-2}) indicates that heat flow is close to the average European value (64 ± 24 mW m^{-2}) and to values obtained in other stable Hercynian provinces of Europe (Čermak, 1979).

HEAT PRODUCTION DATA

In continents, the thermal regime of the crust is closely related to the nature and distribution of heat sources. Moreover, in some stable areas of the world, a linear relationship exists between surface heat flow and surface heat production (Birch et al., 1968). Therefore, it is important to study the surface heat production in order to evaluate the contribution of heat sources to the surface heat flow. Heat production is calculated from uranium, thorium and potassium concentrations according to the work of Birch (Birch et al., 1968). In the present work, new measurements from the Maures and Estérel are presented and compared with previous results from Corsica.

Surface geology

The Hercynian basement outcropping in the Maures and Estérel, mostly formed by metamorphic rocks, is different from the basement outcropping in Corsica, mostly formed by Hercynian granites. The Maures–Estérel province is characterized by two Paleozoic metamorphic units, the Maures in a southwestern position and the Tanneron in a northeastern position (Fig. 5). These two massifs are separated by the Permian volcanic and sedimentary unit of the Estérel. The petrographic features of the metamorphic basement have been studied by Caruba (1983) and Crevola (1977). The western part of the Maures is mostly formed by micaschist and two-mica gneiss intruded by Cambrian granite–gneiss. The eastern part of the Maures and the Tanneron massif are formed by other metamorphic rocks, mostly anatectic gneiss, also intruded by Cambrian granite–gneiss. These two metamorphic domains are separated by a N–S fault along which the Hercynian granite of Plan De La Tour is situated (Fig. 5). Permian rhyolites correspond to the Estérel massif sensu stricto. A granitic equivalent of these rhyolites was found as xenoliths in the Oligocene Estérellite (microdiorite).

Corsica is classically divided into two parts: Alpine Corsica on the western part of the island, which corresponds to the obduction of a Mesozoic unit during the Middle Cretaceous, and Hercynian Corsica on the western and southern parts, formed by the Hercynian and Permian granitic basement. Hercynian granites belong to two magmatic associations, the calk-alkaline and the sub-alkaline types.

Permian granites represent anorogenic types associated with the rhyolites in the northern part of the island, but not in the southern part. This suggests that the level of erosion is increasing from Estérel (rhyolites outcrop and granites exist at deeper levels) to the north of Corsica (both rhyolites and granites outcrop) and finally, to the south of Corsica (only granites exist) (Bonnin and Orsini, 1980; Vellutini, 1977).

Heat production data from the Maures and Estérel

U, Th and K concentrations have been determined by Epithermal Neutron Activation Analysis (ENAA) and compared, for a few samples, to measurements obtained by Gamma-Ray Spectrometry (GRS); the difference is generally lower than 10%, which is acceptable for this heat production study. Samples are representative of the different geological formations (Fig. 6), and results are presented in

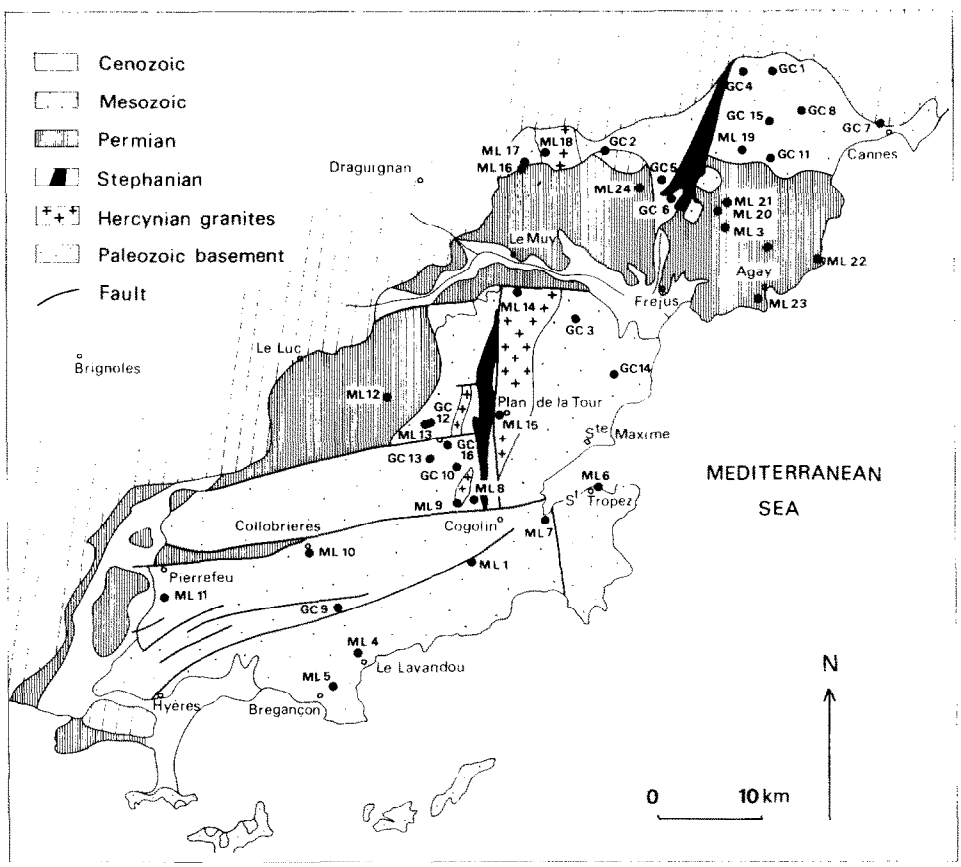

Fig. 6. Geological map of Maures and Estérel and location of samples analyzed for U, Th and K.

Table 3 with average values for each petrologic type. Metamorphic rocks are classified in two categories: metasedimentary rocks (micaschist, gneiss and anatectic gneiss) and granite–gneiss. The radiogenic content does not significantly change with the grade of metamorphism for metasedimentary rocks (Table 3) and average heat production is $2.1 \pm 0.7\,\mu W\ m^{-3}$. Granite–gneiss has a higher average U content

TABLE 3

Heat production data from Maures–Estérel

	$U \pm \sigma_U$ (ppm)	$Th \pm \sigma_{Th}$ (ppm)	$K \pm \sigma_K$ (%)	$A \pm \sigma_A$ ($\mu W\ m^{-3}$)	Th/U	Method *	Standard
Granite gneiss							
Average	4.43 2.01	13.71 4.09	3.06 0.53	2.44 0.64	3.68		
ML 4	5.33 0.31	19.19 0.40	3.53 0.16	3.12 0.09	3.60	GRS	3V61
	5.79 0.04	21.11 0.55	3.61 0.05	3.38 0.04	3.65	ENAA	GSN
GC 5	7.70 0.04	10.06 0.07	3.07 0.17	3.03 0.02	1.31	ENAA	GSN
GC 10	2.84 0.03	11.69 0.08	2.28 0.14	1.80 0.02	4.12	ENAA	GSN
GC 15	2.44 0.03	15.07 0.05	3.67 0.10	2.08 0.01	6.18	ENAA	GSN
GC 16	3.37 0.02	10.61 0.05	2.68 0.12	1.90 0.01	3.15	ENAA	GSN
Granite							
Average	7.20 3.09	10.59 3.08	3.88 0.22	3.02 0.74	1.93		
ML 6	10.54 0.57	6.30 0.18	4.16 0.18	3.61 0.15	0.60	GRS	3V61
	10.34 0.05	5.70 0.22	4.14 0.21	3.51 0.03	0.55	ENAA	GSN
ML 8	4.51 0.15	14.88 0.28	3.64 0.06	2.60 0.04	3.30	ENAA	GSN
ML 14	7.24 0.15	12.58 0.31	3.85 0.15	3.17 0.05	1.74	ENAA	GSN
ML 15	3.05 0.03	9.51 0.23	3.66 0.25	1.84 0.03	3.12	ENAA	GSN
ML 18	11.53 0.04	11.30 0.26	4.45 0.13	4.25 0.02	0.98	ENAA	GSN
	10.85 0.11	10.30 0.23	4.13 0.05	3.97 0.03	0.95	ENAA	GSN
Diorite							
Average	1.71 0.81	5.45 2.53	1.73 0.30	1.00 0.43	3.20		
ML 23	0.90 0.01	2.91 0.01	1.43 0.09	0.58 0.01	3.23	ENAA	GSN
ML 17	3.51 0.21	6.33 0.17	1.80 0.09	1.55 0.06	1.80	GRS	3V61
	2.52 0.02	7.98 0.31	2.02 0.04	1.43 0.02	3.17	ENAA	GSN
Rhyolite							
Average	6.19 0.73	17.49 6.61	4.80 2.67	3.34 0.57	2.86		
ML 16	5.44 0.04	11.28 0.06	4.79 0.17	2.70 0.02	2.07	ENAA	GSN
ML 21	5.89 0.01	25.12 0.05	7.58 0.14	4.08 0.01	4.26	ENAA	GSN
ML 22	6.27 0.01	20.85 0.02	1.19 0.06	3.25 0.01	3.33	ENAA	GSN
ML 24	7.15 0.02	12.7 0.06	5.64 0.24	3.33 0.02	1.78	ENAA	GSN
Micaschist							
Average	3.64 0.08	22.14 1.10	3.79	2.91 0.08	6.09		
GC 13	3.71 0.03	22.91 0.50	3.79 0.06	2.99 0.04	6.18	ENAA	GSN
ML 11	3.56 0.04	21.36 0.38	3.78 0.21	2.83 0.04	6.00	ENAA	GSN

TABLE 3 (continued)

	$U \pm \sigma_U$ (ppm)	$Th \pm \sigma_{Th}$ (ppm)	$K \pm \sigma_K$ (%)	$A \pm \sigma_A$ ($\mu W\ m^{-3}$)	Th/U	Method *	Standard
Gneiss							
Average	3.22 1.14	13.95 4.69	2.91 0.73	2.13 0.63	4.62		
ML 1	3.34 0.21	22.43 0.46	4.75 0.20	2.95 0.07	6.70	GRS	3V61
	3.66 0.10	20.43 0.37	4.03 0.10	2.82 0.04	5.58	ENAA	GSN
ML 9	3.23 0.03	10.81 0.06	2.60 0.16	1.87 0.02	3.35	ENAA	GSN
GC 14	2.05 0.01	17.08 0.05	2.30 0.05	1.99 0.01	8.33	ENAA	GSN
	2.20 0.01	18.41 0.04	2.63 0.12	2.15 0.01	8.37	ENAA	GSN
ML 10	0.56 0.03	3.09 0.22	1.96 0.13	0.56 0.02	5.52	ENAA	GSN
ML 13	4.27 0.02	15.55 0.06	3.09 0.18	2.53 0.02	3.64	ENAA	GSN
GC 4	3.78 0.04	11.93 0.07	2.64 0.08	2.10 0.01	3.16	ENAA	GSN
GC 6	3.47 0.02	15.28 0.06	3.07 0.13	2.30 0.01	4.40	ENAA	GSN
GC 9	2.85 0.03	12.51 0.07	3.45 0.04	1.98 0.01	4.39	ENAA	GSN
GC 11	3.24 0.03	13.11 0.52	1.67 0.04	1.95 0.04	4.05	ENAA	GSN
GC 12	4.96 0.03	18.37 0.08	3.93 0.21	3.00 0.02	3.70	ENAA	GSN
Anatectic gneiss							
Average	3.76 0.25	11.27 2.79	3.32 1.02	2.20 0.60	3.03		
ML 7	3.46 0.02	12.55 0.04	2.21 0.10	2.02 0.01	3.63	ENAA	GSN
ML 19	6.03 0.34	19.31 0.40	3.88 0.17	3.34 0.09	3.20	GRS	3V61
	4.85 0.11	15.87 0.27	3.50 0.06	2.75 0.04	3.27	ENAA	GSN
GC 1	4.65 0.03	10.65 0.32	4.20 0.08	2.39 0.03	2.29	ENAA	GSN
GC 2	2.35 0.02	7.60 0.04	1.52 0.03	1.31 0.01	3.23	ENAA	GSN
GC 3	4.00 0.02	13.99 0.22	4.66 0.05	2.50 0.02	3.50	ENAA	GSN
GC 7	2.86 0.09	8.44 0.20	3.50 0.09	1.69 0.03	2.95	ENAA	GSN
GC 8	4.13 0.04	9.77 0.07	3.67 0.15	2.14 0.02	2.37	ENAA	GSN

* GRS = gamma-ray spectrometry; ENAA = epithermal neutron activation analysis.

and consequently a higher heat production ($2.4 \pm 0.6\ \mu W\ m^{-3}$). In a similar work in the Massif Central (France), Lucazeau and Vasseur (1981) have found values in the same range. Surface anatectic gneiss of the Massif Central has a heat production of $1.91\ \mu W\ m^{-3}$ whereas the same material erupted from a depth of 20 km during recent volcanism, has a heat production of $1.89\ \mu W\ m^{-3}$. In other geological provinces of the world, similar considerations apply (Smithson and Decker, 1974; Jaupart et al., 1982).

Granites of the Maures and Estérel are close to the leucogranite type of the Massif Central (Lucazeau and Vasseur, 1981), with low Th and Th/U values, characteristic of granites of crustal origin. Heat production of these granites is $3.0 \pm 0.7\ \mu W\ m^{-3}$. The sensu stricto massif of Estérel is formed by Permian rhyolites. Heat production of these rocks is $3.3 \pm 0.6\ \mu W\ m^{-3}$. Finally, diorites have a low heat production ($1.0\ \mu W\ m^{-3}$) and only represent small outcropping volumes.

TABLE 4

Apatite fission track data from the Maures and Estérel (ML 17, ML 6 and ML 4) and from Corsica (Mailhé, 1986)

Sample *	Mineral	Fossil		Induced		Neutron dose ($\times 10^{15}$ n/cm^2)	Age $\pm 1\sigma$ (Ma)	Number of grains or fields	ξ [c]
		Tracks ($\times 10^5$/cm^2)	Tracks [b]	Tracks $\times 10^5$/cm^2	Tracks [b]				
ML 17	apatite	3.68	4226	6.45	5694	4.00	135.2 ± 6.1 [p]	134f/108i	0.040
ML 6	apatite	7.67	7252	15.45	10042	4.00	117.7 ± 4.3 [p]	109f/76i	0.044
ML 4	apatite	0.54	261	1.52	507	4.00	85.1 ± 13.1 [p]	72f/50i	0.114
A (ns)	apatite	0.8695	65	2.238	80	4.29	99.0 ± 18.3	23f/11i	0.154
(290)	apatite	0.4615	36	1.0678	59	4.29	110.0 ± 20.2	24f/17i	0.105
(300)	apatite	0.4061	33	1.046	51	4.29	98.9 ± 17.5	25f/15i	0.070
B (ns)	apatite	1.114	114	1.92	164	0.8074	28.0 ± 4.1	50f/44i	0.093
(ns) [d]	apatite	1.13	94	1.58	93	0.8074	34.5 ± 4.4	41f/29i	0.085
C (ns)	apatite	0.615	80	1.076	63	0.8074	27.6 ± 4.3	40f/18i	0.114
D (ns)	apatite	2.613	119	3.02	84	0.8074	41.7 ± 6.0 [p]	40f/18i	0.109
E1 (ns)	apatite	0.384	91	1.3	215	2.29	40.4 ± 4.5	73f/51i	0.080
(290)	apatite	0.1905	26	0.6474	101	2.29	40.2 ± 6.6	42f/48i	0.075
(300)	apatite	0.1487	29	0.4886	81	2.29	41.6 ± 7.8	60f/51i	0.085
E2 (ns)	apatite	0.285	76	1.055	120	2.29	36.9 ± 4.7	82f/35i	0.072

(290)	apatite	0.224	51	0.69	101	2.29	44.3 ± 7.6	70f/45i	0.072
(300)	apatite	0.1445	31	0.4835	77	2.29	40.8 ± 8.8	66f/49i	0.096
F (ns)	apatite	1.727	83	2.81	155	0.8074	29.6 ± 4.1 [p]	35f/36i	0.093
H (ns)	apatite	1.079	71	1.2	68	0.8074	43.3 ± 7.4 [p]	54f/48i	0.122
I (ns)	apatite	1.35	48	1.92	37	0.8074	33.9 ± 7.5 [p]	25f/15i	0.311
J (300)	apatite	0.13	19	0.232	34	0.8074	29.2 ± 7.6	45f/45i	0.174
P (ns)	apatite	1.45	109	1.81	124	0.8074	38.6 ± 5.1 [p]	32f/31i	0.094
Q (ns)	apatite	2.57	151	2.65	153	0.8074	43.4 ± 5.0 [p]	29f/28i	0.142
(ns) [d]	apatite	2.264	165	2.44	143	0.8074	44.7 ± 5.2 [p]	31f/28i	0.130
FC 3 [e]	apatite	0.22	167	0.82	530	1.62	26.2 ± 2.3 [p]	109f/78i	0.057

$\lambda_F = 7.03 \times 10^{-17}$ yr^{-1}; $^{235}U/^{238}U = 7.252 \times 10^{-3}$; $\sigma_f = 580 \times 10^{-24}$ cm^2.

[a] For apatite: ns = natural state, without laboratory annealing, 290 = one hour laboratory annealing at 290 °C, 300 = one hour laboratory annealing at 300 °C.

[b] Number of tracks actually counted.

[c] ξ = relative standard error of the mean for the induced-track count in apatite.

[d] Counted by observer other than D.M.

[e] Fish Canyon age standard counted at the same time as the samples.

[p] Error calculated from the Poisson relative standard error of mean.

Previous heat production data from Corsica

These data have been published by Lesquer et al. (1983), but it is interesting to recall their principal results in order to discuss heat flow data. The calc-alkaline granites represent about three-thirds of the outcrops in Hercynian Corsica. They are obviously depleted in uranium (1.9 ± 0.7 ppm) as Th/U is very high (7.3). Heat production is only 1.8 ± 0.2 $\mu W\ m^{-3}$. Similar granites in the Massif Central have a higher average uranium content (5.2 ppm) and a Th/U ratio of about 4 (Lucazeau and Vasseur, 1981), consistent with the Th/U expected for granites. Granites of Corsica are therefore probably depleted because of some weathering process.

The leucocratic granites represent evolved members of the calk-alkaline series. They are enriched in uranium (U = 10.4 ppm) and have a high heat production (4.4 ± 0.6 $\mu W\ m^{-3}$). The sub-alkali granites are enriched in uranium (7.6 ppm) and thorium (38 ppm). They consequently have a high heat production (4.9 $\mu W\ m^{-3}$). These values are close to the average values for similar granites in the Massif Central. Finally, the heat production of Permian anorogenic granites vary from 3.0 to 5.3 $\mu W\ m^{-3}$.

APATITE FISSION TRACK (FT) DATA

Fission tracks represent daughter products of the disintegration of ^{238}U and can be used as a dating method. The special feature of this method is that the closure of the system is strongly sensitive to temperature. This closure temperature is a characteristic of minerals, and for apatites, is about 100°C. Therefore, this could be an excellent indicator of paleogeothermal conditions, as apatite FT ages represent the last cooling below 100°C, corresponding to a depth of about 3 km.

In the present study, two sets of data were used: measurements from Corsica published by Mailhé (1986) together with zircon FT data; three new apatite FT ages from the Maures and Estérel, simultaneously determined with the international standard Fish Canyon Tuff complete the previous data. Results are presented in Table 4 and Fig. 7, in which Corsica is drawn in its pre-Oligocene position. More information about the method and references can be found in Mailhé (1986).

The Alpine part of Corsica is characterized by Eocene–Oligocene apatite FT ages (40–30 Ma) whereas the northwest part of the island and the Maures and Estérel give Cretaceous ages. Mailhé (1986) and Mailhé et al. (1986) interpreted fission track data in the eastern part of Corsica assuming differential erosion subsequent to the well-known Eocene compressional stage, with erosion rates of as high as 1 mm yr^{-1}. On the other hand, the western part of Corsica, the Maures and Estérel, and probably the region between them, have only been affected by the Cretaceous phase of the Alpine orogeny, as shown by older apatite ages. This indicates that no erosional process occurred between the Middle Cretaceous and the Oligocene rifting. There is no geological evidence for distention in this area before the

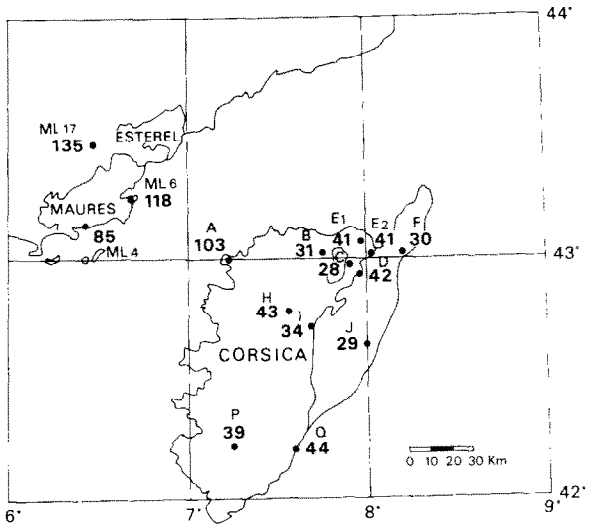

Fig. 7. Apatite fission track data in the Maures and Estérel and in Corsica. The Provençal coastline is in its present-day position whereas Corsica has been replaced in its supposed pre-Oligocene position (after Le Douaran et al., 1984 and Burrus, 1984).

Oligocene. Therefore, except in Alpine Corsica, the thermal regime of the Hercynian crust at the onset of Oligocene rifting was probably in equilibrium.

DISCUSSION

Results presented in the previous sections indicate that the surface heat flow is significantly lower in the Maures and Estérel (58 mW m^{-2}) than in Corsica (76 mW m^{-2}). Moreover, previous work in Sardinia (Loddo et al., 1982) has shown that heat flow is generally low (58 ± 15 mW m^{-2}) except in the Quaternary graben of Campidano (127 ± 43 mW m^{-2}). It is important to explain the origin of the higher value in Corsica in order to understand the thermal structure within and around the Provençal Basin.

Role of heat production

Heat production of granites in Corsica presents a wide range of values from 1.8 μW m^{-3} to 5.3 μW m^{-3}. The lower boundary can be increased to about 3 μW m^{-3} (value of similar granites in the Massif Central), since Corsican calk-alkaline granites are probably depleted in uranium. The difference between surface heat flows could then be explained by 18 km more of calk-alkaline granite or 6 km more of enriched granite in Corsica, relative to the metamorphic basement in the

Maures-Estérel. This explanation is problematic, however, as surface granites are not associated with a heat flow anomaly in Sardinia and as granites presumably exist as well at deeper levels in the Maures and Estérel. It is more likely that the radiogenic heat contribution of the crust in these three areas is roughly the same and that the heat flow anomaly of Corsica has another origin.

Role of erosion

Corsica has been affected by the Alpine orogeny during two major phases: the middle Cretaceous phase, which corresponds to the obduction process, and the Eocene phase, which corresponds to the main tectonic compression. Mailhé et al. (1986) attempted to derive erosion rates from combined fission track data (zircons and apatites) and thermal modelling. Maximum erosion rates during the Eocene phase are observed in Alpine Corsica and are less than 1 mm yr^{-1}. At the present, this yields a maximum heat flow anomaly of less than 10 mW m^{-2}, but for the erosion rates which prevailed in central and western Corsica, no increase in surface heat flow expected. Therefore, erosion could explain heat flow differences between Alpine and Hercynian Corsica, but in no case the differences between Corsica and the Maures, Estérel and Sardinia.

A deep-seated thermal anomaly?

The formation of the Provençal Basin since the Oligocene could have affected the thermal regime of Corsica and increased the surface heat flow. In order to investigate this possibility, it is necessary to gather heat flow data for a wider domain than the Hercynian outcrops. Available data in the Provençal Basin (Foucher and Tisseau, 1984; Burrus and Foucher, 1986), in the Tyrrhenian Sea (Della Vedova et al., 1984; Hutchinson et al., 1985), in Sardinia (Loddo et al., 1982), in Italy (Loddo and Mongelli, 1979), in France (Vasseur, 1982) as well as data presented in this paper, have been used to draw a contour map of heat flow in the Western Mediterranean with an automatic method (Fig. 8). Data have been preliminarily interpolated using a 250 km window because of the nonuniform data distribution, and this map therefore only represents the regional trends.

The Hercynian domain is characterized by a low heat flow (around 60 mW m^{-2}), except in Corsica. Within the Provencal Basin, there is a high heat flow anomaly ($\geqslant$ 90 mW m^{-2}) which extends from Tuscany to the Balearic Basin. This anomaly is not directly connected to the oceanic domain but more likely corresponds to the margins of Corsica and Sardinia. The Gulf of Lions is characterized by a low heat flow (60–70 mW m^{-2}) which can be explained by the blanketing effect of the sediments, which absorbs about 30% of the surface heat flow (Lucazeau and Le Douaran, 1985). A major feature of this map is, therefore, the asymmetric distribution of heat flow within the Provençal Basin.

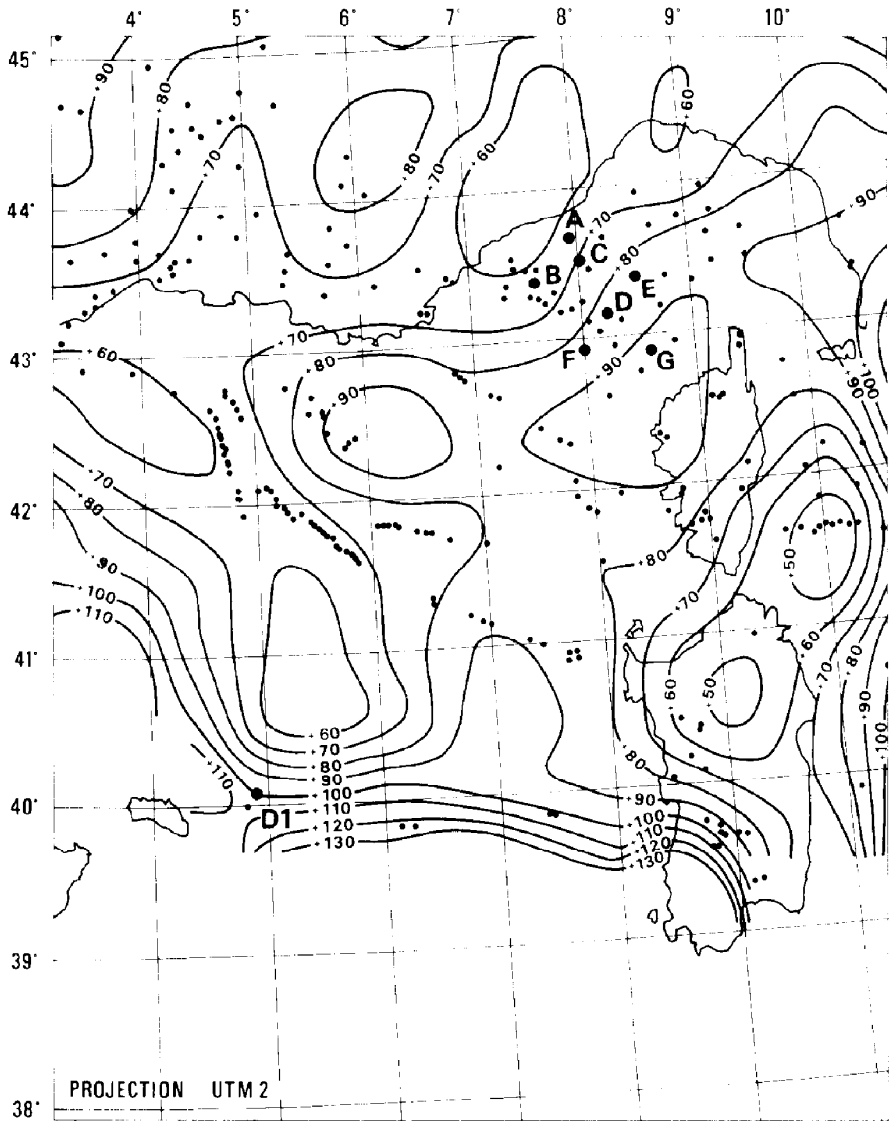

Fig. 8. Heat flow map of the Provençal Basin. Isovalues are mW m^{-2}. Large points correspond to new measurements (uncorrected (uc) for sedimentation effects): *D*1 $Q_{uc} = 92 + 10$ mW m^{-2} (Hutchison et al., 1985); *A* $Q_{uc} = 65 \pm 24$ mW m^{-2} (Jemsek et al., 1985); *B* $Q_{uc} = 56 \pm 7$ mW m^{-2} (Jemsek et al., 1985); *C* $Q_{uc} = 71 \pm 13$ mW m^{-2} (Jemsek et al., 1985); *D* $Q_{uc} = 78 \pm 13$ mW m^{-2} (Jemsek et al., 1985); *E* $Q_{uc} = 103 \pm 3$ mW m^{-2} (Jemsek et al., 1985); *F* $Q_{uc} = 105 \pm 21$ mW m^{-2} (Jemsek et al., 1985); *G* $Q_{uc} = 86 \pm 11$ mW m^{-2} (Jemsek et al., 1985).

Other geological and geophysical anomalies also indicate that the two opposite margins of this Basin are different. Le Douaran et al. (1984) have shown using ESP seismic refraction techniques that the Corsican margin is more extended than the

Provençal margin. Burrus (1984), using combined results of ESP surveys and magnetics, proposed an asymmetric model of oceanic accretion, with greater spreading rates towards Provence. Refraction seismic data on land (Hirn and Sapin, 1977; Egger et al., 1985) and gravity data (Bayer et al., 1976) have shown that the continental crust is 30 km thick beneath Corsica and Sardinia, but thinned beneath the northwestern part of Corsica to about 25 km. This supports the observations of Le Douaran et al. (1984), as do the asymmetric shapes of bathymetry (Réhault, 1981) and the Bouguer anomaly (Morelli et al., 1977), which indicate higher extension on the Corsican margin. These different anomalies indicate an asymmetric structure of the Provençal Basin.

Burrus et al. (1985) and Burrus and Foucher (1986) proposed that a deep-seated thermal anomaly is located beneath the Corsican margin; according to the heat flow map (Fig. 8), this anomaly extends to Tuscany and to the Balearic Basin and could be a residual thermal anomaly related to the paleo-ridge. This hypothesis could also explain how high relief in Corsica (up to 3000 m) can be associated with a normal or thin crust. On the other hand, it apparently contradicts surface-wave studies (Panza et al., 1980), which predict a thick lithosphere in this area. However, the higher heat flow in Corsica is a consequence of the recent evolution of the Western Mediterranean.

Model of initial thermal state

In previous sections, it has been shown that the Hercynian crust around the Provençal Basin, except in Corsica, is characterized by a low heat flow (around 60 mW m^{-2}), which probably corresponds to the equilibrium value of the stable Hercynian domain. It is interesting to study what the possible contributions of the crust and of the mantle to this surface heat flow are, as it is necessary to estimate initial and boundary conditions in thermal modelling. The present day thermal state of the Maures and Estérel, where reliable heat flow and heat production data are available, can be used for this estimate.

A possible way is to derive the crustal radioactivity distribution from seismic crustal reflectors. Rybach (1979) suggested that heat production could exponentially depend on the P-wave velocity. In fact, however, upper crustal rocks have a wide range of heat production values (1–10 μW m^{-3}) but P-wave velocities range from only 6.0 to 6.4 km s^{-1}. On the other hand, rocks from the lower crust have a narrow range of heat production values (0.1–0.3 μW m^{-3} for basic rocks and 1.0–1.5 μW m^{-3} for acidic rocks) whereas P-wave velocities range from 6.6 to 7.4 km s^{-1}.

Few seismic data are available in the Maures and Estérel. After Recq (1970), crustal thickness is 28–30 km along the coastline of the Maures and increases northwards to 34–36 km in the calcareous Provence. Recent surveys along the Ligurian coastline (Thouvenot et al., 1985) and across the Gulf of Genova (Ginzburg et al., 1985) have shown that the crust is formed by two 15 km thick seismic

layers: the P-wave velocity is 6.0 km s^{-1} for the upper layer and 6.6 km s^{-1} for the lower layer. From seismic data on the margin (Le Douaran et al., 1984), the continental crust is thinned but the two layer structure is conserved: at ESP 225 (the closest to the Maures), the thickness of the stretched crust is 16 km with a P-wave velocity of 6.1 km s^{-1} in the 8 km thick upper crust and 7.6 km s^{-1} in the 8 km thick lower layer. This structure is similar to those observed in other parts of the Hercynian domain of France (Hirn, 1980), especially in the outer parts of the Massif Central (Perrier and Ruegg, 1973). As there is strong evidence that Hercynian structures continue from the Massif Central to the Maures and Estérel, information about the deep crust available in the Massif Central from xenoliths carried up by the recent volcanism can be reasonably used in the Maures and Estérel.

Average heat production of the upper crust is estimated from surface rocks. According to Smithson and Decker (1974), this layer is formed by a complex consisting mainly of metamorphic rocks, mixed with granites in the upper part. The bulk of the granites is difficult to evaluate. Enriched granites must generally be thin as they are not associated with a negative gravity anomaly or a higher heat flow in either the Massif Central (Lucazeau and Vasseur, 1981) or Corsica (this study). On the other hand, thicker granites have a lower heat production of 3 μW m^{-3}. Therefore, compared to the metamorphic basement (2 μW m^{-3}), such granites contribute an additional 1 mW m^{-2} km^{-1} or less (due to lateral heat transfer; Jaupart, 1983) to surface heat flow. For the purpose of this model, the effects of granites can be neglected; heat production of the metamorphic basement, which is relatively uniform from the surface to deeper levels (Lucazeau and Vasseur, 1981), is attributed to this upper part of the crust. This part contributes about 30–34 mW m^{-2} to the surface heat flow assuming average heat production is 2–2.25 μW m^{-3}.

In the lower crust, average heat production ranges between 0.3 and 0.8 μW m^{-3} (Lucazeau and Vasseur, 1981). This corresponds to a contribution of 5–12 mW m^{-2} to the surface heat flow. Therefore, mantle heat flow beneath the stable Hercynian crust ranges from 14 to 25 mW m^{-2}; this result is in agreement with global heat flow studies which predict a mantle heat flow beneath stable provinces of about 21–27 mW m^{-2} (Sclater et al., 1980). The average heat production of the crust is 1.1 to 1.5 μW m^{-3}; this result can be compared to geochemical models which predict 0.5 to 1.0 μW m^{-3} (appendix 1, Jaupart and Provost, 1985). Finally, the temperature at the Moho can be calculated on the basis of the distribution of heat sources: it ranges between 375°C ($K = 3$ W m^{-1} °C^{-1}) and 450°C ($K = 2.5$ W m^{-1} °C^{-1}) assuming a constant conductivity (K) in the crust, and between 420°C ($K = 3$ W m^{-1} °C^{-1}) and 500°C ($K = 2.5$ W m^{-1} °C^{-1}) assuming that thermal conductivity decreases with increasing temperature according to the model of Wells (1980).

CONCLUSIONS

The thermal structure of the Western Mediterranean is difficult to understand as it represents the interaction of different time dependent processes. This part of the

Mediterranean Sea is still evolving and thermal modelling is necessary to estimate the temperature field and the mantle heat flow, which is the final goal of thermal studies in the EGT programme. This modelling work requires the establishment of a reference thermal state in order to estimate initial and boundary conditions.

In this paper, we have studied the Hercynian area outcropping around the Provençal Basin in order to propose a reference thermal state in the Western Mediterranean Sea. We believe that, except in Corsica, these areas are presently at thermal equilibrium. The Maures and Estérel, where reliable heat flow and heat production data are available, have been used to study the thermal state of the crust in an area expected to correspond to stationary conditions. The surface heat flow is about 60 mW m^{-2} and the crustal heat contribution, estimated using seismic data, ranges from 35 to 45 mW m^{-2}. Mantle heat flow is therefore 20 ± 5 mW m^{-2}, which is in agreement with general considerations on stable tectonic provinces. The temperature at the Moho is 440 ± 65 °C.

On the other hand, the Hercynian batholith of Corsica has been affected by the Alpine orogeny and subsequent erosion, but also by a deep-seated thermal anomaly evidenced by different geological and geophysical anomalies. The heat flow map for the Western Mediterranean, resulting from a compilation of all existing data, reveals that this deep-seated anomaly extends from Tuscany to the Balearic Basin and could correspond to the paleo-ridge.

ACKNOWLEDGEMENTS

This work was financially supported by "ATP Transferts". It would not have been possible without Alain Lesquer, who made measurements in Corsica and provided us with valuable comments. We also thank Gilbert Crevola, who provided us with gneiss samples from Tanneron. Heat flow measurements have been made owing to the help of Mr. Pasquier from "Service d'aménagement des eaux de Bastia", Mr. Lemperierre, Mr. Tapoul from "Direction Départementale de l'Agriculture de Draguignan", and Mr. Arnaud and Mr. Rippert from COGEMA. We thank too Jean Louis Reyes and Philippe Bonté for providing gamma counting facilities at CFR, Gif. This paper was critically reviewed by Claude Jaupart and another anonymous reviewer. Guy Vasseur critically read the second version of this paper.

REFERENCES

Balling, N., Haenel, R., Ungemach, P., Vasseur, G. and Wheildon, J., 1981. Preliminary guidelines for heat flow density determination. Publication of the Commission of the European Communities, 32 p.

Bayer, M., Bayer, R. and Lesquer, A., 1976. Quelques remarques sur la structure géologique de la Corse d'après la Gravimétrie et le magnétisme. Bull. Soc. Géol. Fr., 28: 1189–1194.

Biju-Duval, B., Letouzey, J. and Montadert, L., 1978. Structure and evolution of the Mediterranean basins. Initial Rep. Deep-Sea Drill. Proj., 42: 951–984.

Birch, F., Roy, F.R. and Decker, E.R., 1968. Heat flow and thermal history in New England and New York. In: E. an-Zen (Editor), Studies of Appalachian Geology. Interscience, New York, N.Y., pp. 437–451.

Bonnin, B. and Orsini, J.B., 1980. Les granitoides de Provençe, du Mercantour et de Corse. In: A. Autran and J. Dercourt (Editors), Evolution Structurale de la France. Congr. Geol. Int., 26e, Coll. C7, Mém. Bur. Rech. Géol. Min. 107: 77–81.

Burrus, J., 1984. Contribution to a geodynamic synthesis of the Provençal basin (North-Western Mediterranean). Mar. Geol. 55: 247–269.

Burrus, J. and Foucher, J.P., 1986. Contribution to the thermal regime of the Provencal Basin based on Flumed heat flow surveys and previous investigations. Tectonophysics, 129 (this vol.): 303–334.

Burrus, J., Foucher, J.P., Avedik, F. and Le Douaran, S., 1985. Deep structure and thermicity of the Provençal basin. In: D.A. Galson and St. Mueller (Editors), Proceedings of the Second Workshop on the EGT Project: The Southern Segment. European Science Foundation, Strasbourg, pp. 183–190.

Caruba, C., 1983. Nouvelles données pétrographiques, minéralogiques et géochimiques dans le massif métamorphique des Maures (Var, France). Thesis, Univ. of Nice, 359 pp.

Čermak, V., 1979. Heat flow map of Europe. In: V. Čermak and L. Rybach (Editors), Terrestrial Heat flow in Europe. Springer, Berlin, pp. 3–40.

Crevola, G., 1977. Etude pétrographique et structurale de la partie orientale du Massif du Tanneron (Provence). Thesis, 3rd cycle, Univ. of Nice, 355 pp.

Della Vedova, B., Pellis, G., Foucher, J.P. and Réhault, J.P., 1984. Geothermal structure of the Tyrrhenian Sea. Mar. Geol., 55: 271–289.

Egger, A., Ansorge, J. and Mueller, St., 1985. Crustal structure of Corsica and the lower lithosphere under the Corsica–Sardinia block. In: D.A. Galson and St. Mueller (Editors), Proceedings of the Second Workshop on the EGT Project: The Southern Segment. European Science Foundation, Strasbourg, pp. 207–214.

Foucher, J.P. and Tisseau, C., 1984. Thermal regime of Atlantic type continental margins: Bay of Biscay and Gulf of Lion. In: B. Durand (Editor), Thermal phenomena in Sedimentary Basins. Technip, Paris, pp. 221–226.

Ginzburg, A., Makris, J. and Nicolich, R., 1985. A seismic refraction profile across the Ligurian Sea. In: D.A. Galson and St. Mueller (Editors), Proceeding of the Second Workshop on the EGT Project: The Southern Segment. European Science Foundation, Strasbourg, pp. 207–214.

Hirn, A., 1980. Le cadre structural profond d'après les profils sismiques. In: A. Autran and J. Dercourt (Editors), Evolution Structurale de la France. Congr. Géol. Int., 26e, Coll. C7, Mém. Bur. Rech. Géol. Min., 107: 34–39.

Hirn, A. and Sapin, M., 1977. Crustal structure beneath Corsica. In: Crustal and upper mantle structure of the Northern Apennines, the Ligurian Sea and Corsica derived from seismic data. Boll. Geofis. Teor. Appl., 75–76: 233–235.

Hutchison, I., Von Herzen, R.P., Louden, K.E., Sclater, J.G. and Jemsek, J., 1985. Heat Flow in the Balearic and Tyrrhenian basins, Western Mediterranean. J. Geophys. Res., 90: 685–701.

Jaupart, C., 1983. Horizontal heat transfer due to radioactivity contrasts: causes and consequences of the linear heat flow relation. Geophys. J.R. Astron. Soc., 75: 411–435.

Jaupart, C. and Provost, A., 1985. Heat focussing, granite genesis and inverted metamorphic gradients in continental collision zones. Earth Planet. Sci. Lett., 73: 385–397.

Jaupart, C., Mann, J.R. and Simmons, G., 1982. A detailed study of the distribution of heat flow and radioactivity in New Hampshire (U.S.A.). Earth Planet. Sci. Lett., 59: 267–287.

Jemsek, J., Von Herzen, R., Réhault, J.P., William, D.L. and Sclater, J., 1985. Heat flow and lithospheric thinning in the Ligurian basin (NW Mediterranean). Geophys. Res. Lett., 12: 693–696.

Le Douaran, S., Burrus, J. and Avedik, F., 1984. Deep structure of the northwestern Mediterranean: a two-ship seismic survey. Mar. Geol., 55: 325–345.

Lesquer, A., Pagel, M., Orsini, J.B. and Bonnin, B., 1983. Premières déterminations du flux de chaleur et de la production de chaleur en Corse. C.R. Acad. Sci. Paris, 297: 491–494.

Loddo, M. and Mongelli, F., 1979. Heat Flow in Italy. In: V. Čermák and L. Rybach (Editors), Terrestrial Heat Flow in Europe. Springer, Berlin, pp. 221–231.

Loddo, M., Mongelli, F., Pecorini, G. and Tramacere, A., 1982. Prime Mesure di Flusso di Calore in Sardegna. CNR-RFE-RP 10: 181–210.

Lucazeau, F. and Le Douaran, S., 1985. The blanketing effect of sediments in basins formed by extension: a numerical model. Application to the Gulf of Lion and Viking graben. Earth Planet. Sci. Lett., 74: 92–102.

Lucazeau, F. and Vasseur, G., 1981. Production de chaleur et régime thermique de la croute du Massif Central. Ann. Géophys., 37: 493–513.

Lucazeau, F., Vasseur, G., Foucher, J.P. and Mongelli, F., 1985. Heat flow along the southern segment of EGT. In: D.A. Galson and St. Mueller (Editors), Proceedings of the Second Workshop on the EGT Project: The Southern Segment. European Science Foundation, Strasbourg, pp. 59–63.

Mailhé, D., 1986. Geodynamic evolution and tectonics of the Alpine orogeny in Corsica (France) in the light of fission track dating. Tectonics, in press.

Mailhé, D., Lucazeau, F. and Vasseur, G., 1986. Uplift history of thrust belts: an approach based on fission track data and thermal modelization. Tectonophysics, 124: 177–191.

Morelli, C., Giese, P., Carrozo, M.T., Colombi, B., Guerra, I., Hirn, A., Letz, A., Nicolich, R., Prodhel, C., Reichert, C., Rower, M., Sapin, M., Scarascia, S. and Wigger, P., 1977. Crustal and upper mantle structure of Northern Apennines, the Ligurian Sea and Corsica derived from seismic and gravimetric data. Boll. Geofis. Teor. Appl., 75–76: 199–260.

Panza, G.F., Mueller, St. and Calcagnile, G., 1980. The gross features of the lithosphere–asthenosphere system in Europe from seismic surface waves and body waves. Pure Appl. Geophys., 118: 1209–1213.

Perrier, G. and Ruegg, J.C., 1973. Structure profonde du Massif Central français. Ann. Geophys., 29: 435–502.

Recq, M., 1970. Courbes d'égale profondeur de la discontinuité de Mohorovičić en Provence. C.R. Acad. Sci. Paris, 270: 11–13.

Réhault, J.P., 1981. Evolution tectonique et sédimentaire du bassin Ligure (Méditerranée Occidentale). Thesis, Univ. of Paris VI, 2 vols.

Rybach, L., 1979. The relationship between seismic velocity and radioactive heat production in crustal rocks: an exponential law. Pure Appl. Geophys., 177: 75–82.

Sclater, J.G., Jaupart, C. and Galson, D., 1980. The heat flow through oceanic and continental crust and the heat loss of the earth. Rev. Geophys. Space Phys., 18: 269–311.

Smithson, S.B., and Decker, E.R., 1974. A continental crust model and its geothermal implications. Earth Planet. Sci. Lett., 22: 215–225.

Thouvenot, F., Ansorge, J. and Eva, C., 1985. Deep structure of the western Alps: new constraints from the EGT-S seismic experiment. In: D.A. Galson and St. Mueller (Editors), Proceedings of the Second Workshop on the EGT Project: The Southern Segment. European Science Foundation, Strasbourg, pp. 109–114.

Vasseur, G., 1982. Synthèse des résultats de flux géothermique en France. Ann. Geophys., 38: 189–201.

Vellutini, P., 1977. Le magmatisme Permien de la Corse du Nord Ouest. Son extension en Méditerranées Occidentale. Thesis, Univ. of Marseille, 277 pp.

Wells, P.R.A., 1980. Thermal models for magmatic accretion and subsequent metamorphism of continental crust. Earth Planet. Sci. Lett., 46: 253–265.